Reactions of Polycarbonate with Cyclohexene Oxide and Phosphites: A Density Functional Study

J. Akola, P. Ballone,† and R. O. Jones*

Institut für Festkörperforschung, Forschungszentrum Jülich, D-52425 Jülich, Germany

Received October 9, 2001; Revised Manuscript Received December 10, 2001

ABSTRACT: Epoxides and phosphites are often used as additives to stabilize the properties of polymers, including bisphenol A polycarbonate (BPA-PC). We describe density functional (DF) calculations of the reactions of cyclohexene oxide (CHO, cyclohexane epoxide) and phosphites with chain segments of BPA-PC, with the aim of identifying possible reaction paths and energy barriers. The reactions of CHO with the OH-terminated PC chains and with the carbonate group are exothermic, although there is an energy barrier in each case of more than 10 kcal/mol. A comparison of results for different CHO isomers demonstrates the importance of steric effects. The reactions between the same groups of the PC chain and the phosphites 2-[2,4-bis(*tert*-butyl)phenoxy]-5,5-dimethyl-1,3,2-dioxaphosphorinane] (BPDD) and trimethyl phosphite (TMP), and their phosphonate isomers are characterized by large energy barriers.

I. Introduction

The prediction of the paths of chemical reactions and the related energy barriers remains a major challenge for computational chemistry. Systems of interest are often far too complex for methods based on the many-electron wave function, while most force field (FF) methods cannot model such processes because they assume a fixed bonding topology. Furthermore, predictions obtained using FF methods that do allow the formation and breaking of chemical bonds are often limited by uncertainties in the choice of parameters involved. In recent years, the density functional (DF) formalism has been the basis of many calculations of molecules and atomic clusters and has provided valuable information and predictions. The present work extends a continuing study of the application of DF calculations to organic molecules and polymers, focusing on bisphenol A polycarbonate (BPA-PC).

BPA-PC is an important thermoplastic that has served as a prototype polymer for both theorists and experimentalists.[1] In earlier work, we have studied the structures and vibration frequencies of its fragments and closely related molecular crystals,[2,3] as well as reactions of nucleophilic molecules (phenol, lithium and sodium phenoxides, and tetraphenylphosphonium phenoxide (PPh_4OPh)) with the cyclic tetramer of PC.[4,5] The local atomic coordination of the cyclic tetramer and the PC chain are very similar, and the calculations have provided a picture of the reaction paths and energy barriers that is consistent with experimental information. In practice, however, the stability of polycarbonate resin to heat, light, and other chemicals must be improved by appropriate additives, especially if extrusion or injection molding is to be used.[6]

There is much empirical information about the effects of polymer additives, examples of which are phosphite and epoxide molecules. These are common building blocks in organic synthesis, and ring-opening of epoxides has been studied on many occasions. Nevertheless, little is known about the atomistic details of their roles as additives. Contributions to the observed effects could arise from (a) reactions occurring in the original system, (b) reactions between this system and the additives, or (c) an inert role of the additives, e.g., as spacers between polymer chains. As a step toward the clarification of such processes, we study here the reactions of isomers of $C_6H_{10}O$ (cyclohexene oxide, CHO, cyclohexane epoxide) and of phosphite molecules with simple PC chains. We compare the reactivity of these molecules at sites in the chain and at defects, exemplified by a phenol-terminated chain. For each molecule and reaction site we study possible reaction mechanisms and energy barriers, the effects of using different reactant isomers, and the role of steric hindrance. Structural trends of the molecules related to CHO (C_6H_nO, $n = 4-10$) are also investigated.

In section II, we outline the method used in the calculations. The properties of the isolated reactant molecules and the course of the reactions are discussed in sections III and IV for cyclohexene oxide and phosphite molecules, respectively. In section V, we summarize our findings.

II. Method of Calculation

The method of calculation has been described in detail elsewhere.[7,8] The electron−ion interaction is represented by ionic pseudopotentials with the (nonlocal) form suggested by Troullier and Martins.[9] We use periodic boundary conditions and an orthorhombic unit cell with lattice constants appropriate for the reaction under consideration. The orbitals are expanded in terms of a plane wave basis (kinetic energy cutoff of 35 au) using a single point ($\boldsymbol{k} = 0$) in the Brillouin zone, and we use the approximation of Perdew, Burke, and Ernzerhof (PBE)[10] for the exchange-correlation energy.

The energy surfaces are studied by adopting a reaction coordinate R_C, e.g., the distance between the C atom of a carbonate group in the ring and the O atom on phenol or phenoxide, which is varied until a structural transformation or a large energy change takes place. For large values of R_C (typically >5 Å), the weak interaction between the reactants means that changes of 1 Å are possible. As the reaction proceeds, progressively shorter steps are necessary. For each value of R_C,

* Corresponding author. E-mail address: r.jones@fz-juelich.de.
† Permanent address: Università degli Studi di Messina, Dipartimento di Fisica, Contrada Papardo, I-98166 Messina, Italy.

10.1021/ma011757t CCC: $22.00 © 2002 American Chemical Society
Published on Web 02/07/2002

Table 1. Bond Lengths (Å) and Angles (deg), Atomic Charges (−*e*), Dipole Moments (D) and Vibrational Frequencies (cm^{-1}) Calculated for the Most Stable Isomers of (a) C_6H_4O, (b) C_6H_6O, (c) C_6H_8O, (d) Cis and (e) Trans Isomers of $C_6H_{10}O$, and (f) Cyclohexane (C_6H_{12}). For notation, see Scheme 1

atoms	a	b	c	d	e	f
C_1-O	1.484	1.452	1.455	1.452	1.465	
C_2-O	1.484	1.452	1.455	1.460	1.466	
C_1-C_2	1.320	1.527	1.474	1.478	1.455	1.534
C_2-C_3	1.360	1.462	1.510	1.517	1.506	1.534
C_3-C_4	1.444	1.359	1.501	1.536	1.593	1.534
C_4-C_5	1.391	1.443	1.337	1.531	1.592	1.534
C_5-C_6	1.443	1.359	1.501	1.533	1.592	1.534
C_6-C_1	1.360	1.462	1.510	1.510	1.503	1.534
C_1-O-C_2	52.8	63.4	60.9	61.0	59.5	
$C_1-C_2-C_3$	127.9	117.1	121.0	121.5	109.5	111.4
$C_2-C_3-C_4$	108.5	120.6	114.1	113.4	100.8	111.4
$C_3-C_4-C_5$	123.6	121.4	124.3	111.9	119.1	111.4
$C_4-C_5-C_6$	123.6	121.4	124.3	110.6	119.0	111.4
$C_5-C_6-C_1$	108.5	120.6	114.1	112.3	101.1	111.4
$C_1-O-C_2-C_3$	2.6	73.4	68.0	67.5	88.0	
$C_1-C_2-C_3-C_4$	0.6	10.0	8.6	10.9	27.8	54.9
$Q(O)$	−0.26	−0.23	−0.31	−0.31	−0.44	
$Q(C_2)$	0.20	0.06	0.04	0.03	0.23	−0.03
$Q(C_3)$	−0.20	−0.13	0.09	0.00	−0.19	−0.03
$Q(C_4)$	−0.14	−0.09	−0.18	−0.03	−0.02	−0.03
dipole	1.77	1.78	1.88	1.913	2.66	0
C−H stretch	3120	3040−3100	2920−3090	2930−3020	2960−3033	2940−3010
C_1-C_2 stretch	1849	1340	1423	1418	1277	
C−O stretch	815	820	858	870	865	
C−O in-plane bend	368	mixed	350	mixed	421	
C−O out-of-plane bend	395	mixed	383	371	380	

Scheme 1. Cyclohexene Oxide

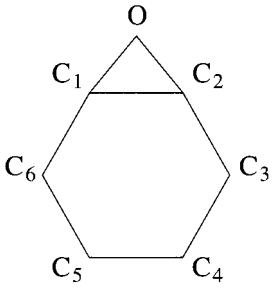

we relax *all* other degrees of freedom of the structure using quenched molecular dynamics,[11] until the energy gradients along the unconstrained directions are less than an appropriate value. In most cases, it is necessary to change the reaction coordinate as the reaction proceeds.

III. Reactions of Cyclohexene Oxide with PC

Published work on the isolated cyclohexene oxide molecule has included microwave[12] and electron diffraction[13] studies, and a recent nuclear magnetic resonance (NMR) study was complemented by Hartree−Fock (HF), second order Møller-Plesset (MP2), and density functional calculations.[14] To characterize CHO, we have calculated its structural and vibrational properties and those of related ring molecules.

A. C_6H_nO Rings, with $n = 4, 6, 8,$ and 10. Cyclohexene oxide $C_6H_{10}O$ may be viewed as a member of a family of ring molecules C_6H_nO ($n = 4, 6, 8, 10$) that shows interesting structural trends. Some of these molecules may react rapidly in air or other environments, but the calculations show that the isolated molecules are all stable. In Figure 1 we show the most stable forms of (a) C_6H_4O and (b) C_6H_6O and four isomers of C_6H_8O (Figure 1c−f), and the structural

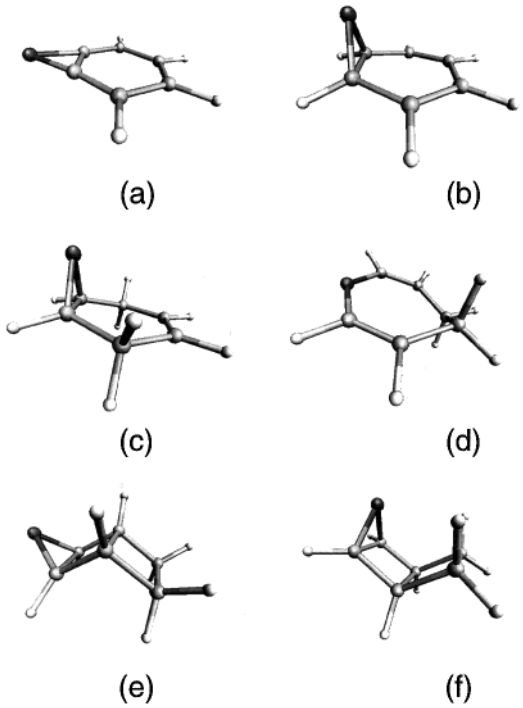

Figure 1. Isomers of (a) C_6H_4O, (b) C_6H_6O, and (c−f) C_6H_8O. C atoms are gray; O, black; and H, white.

parameters of the most stable isomers in C_6H_nO, $n = 4$, 6, and 8, are given in Table 1.[15] The most stable C_6H_8O isomer (Figure 1c) has C_2 symmetry, but the isomer shown in Figure 1d is only 1.3 kcal/mol higher in energy. This near-degeneracy indicates the delicate energy balance between the formation of the epoxy ring and the ring twist evident in Figure 1d. The energies of the exo-boat (Figure 1e) and endo-boat (Figure 1f) structures lie 31 and 38 kcal/mol, respectively, above that of the most stable isomer.

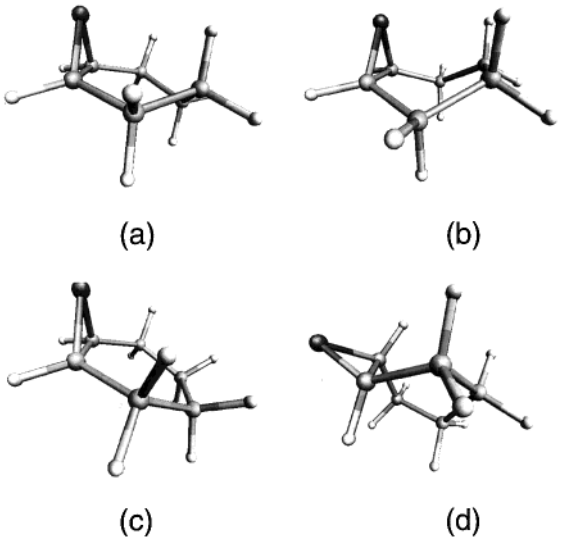

Figure 2. Isomers of cyclohexene oxide CHO. C atoms are gray; O, black; and H, white.

The most stable isomer of cyclohexene oxide $C_6H_{10}O$ (the cis structure shown in Figure 2a) shows the ring twist also seen in Figure 1d. Calculated and experimental structural parameters and selected vibration frequencies are given in Table 1, column d. There is very good agreement between the calculated structural parameters and those found in the analysis of electron diffraction data,[13] with calculated bond lengths and bond angles differing from measured values by less than 0.01 Å and 1°, respectively. A second enantiomeric structure, found by ring-inversion via the endo-boat structure (Figure 2b), is only 4.3 kcal/mol higher. This energy difference agrees remarkably well with the estimates of the free energy barrier from dynamic NMR spectroscopy (4.3 ± 0.2 kcal/mol).[14] The exo-boat structure shown in Figure 2c is an additional 6 kcal/mol higher in energy. The trans form (Figure 2d, structural parameters in Table 1, column e) has considerable strain in the neighborhood of the epoxy ring and an energy 41 kcal/mol above that of the cis isomer.

The high reactivity of epoxides and their widespread use as organic reagents arise from the strain in the three-membered ring. An indication of this can be found by computing total energies for the reaction of CHO with H_2 leading to cyclohexane and O_2:

$$C_6H_{10}O + H_2 \rightarrow C_6H_{12} + \frac{1}{2}O_2$$

The calculations indicate that the reaction is exothermic (approximately 6 kcal/mol), and similar potential energy differences are found in all of the reactions between $C_6H_{10}O$ and PC described below. This shows that the reactions will occur spontaneously unless prevented by kinetic barriers.

B. Reaction of Cyclohexene Oxide with PC. In earlier work we used the phenol-terminated segment ("DPC-plus") as a model for PC in reactions with PPh_4OPh,[5] and we studied the reactions with two points of the chain: (a) the OH termination and (b) the carbonate group. Reactions with the same segments of the PC chain are performed here in each case for the cis isomer (Figure 2a) and the less stable—and presumably more reactive—trans isomer (Figure 2d) of cyclohexene oxide.

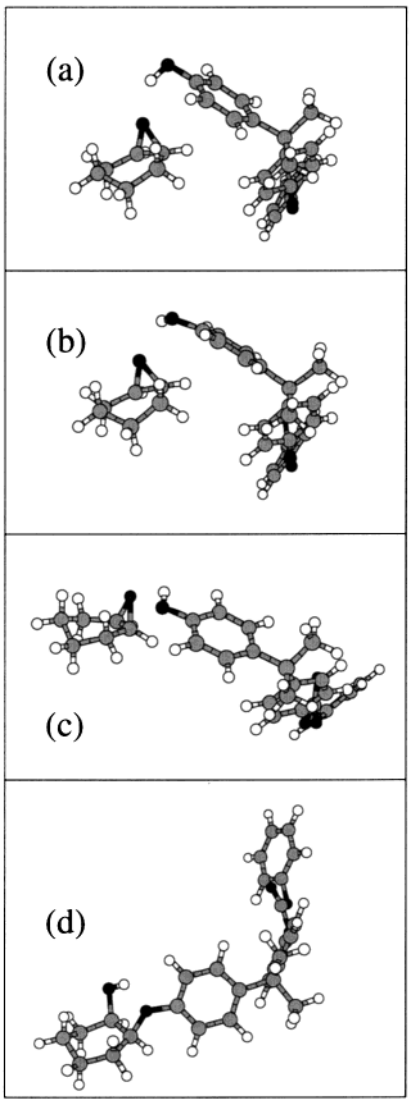

Figure 3. Reaction of the cis isomer of CHO with end of phenol-terminated PC chain.

1. Cis Isomer of CHO (Figure 2a). The reaction of CHO with the OH termination of a PC unit can be seen as an example of the acid-catalyzed cleavage of the epoxy ring, whose general features are discussed in standard textbooks.[16] However, the complexity and low acidity of PC raise the energy barrier to reaction well above the values estimated for other molecules involving CHO.[17]

The calculations begin with two well-separated molecules with a total energy equal to the sum of the energies of the components (referred to as the energy zero in the following). The course of the reaction is shown in Figure 3. At first we reduce the separation R_{O-O} between the O atoms in the OH termination and in the epoxy ring. The energy of the system changes little until R_{O-O} approaches ~3 Å, when the proton in the OH group points toward the epoxy O. This suggests the formation of a very weak hydrogen bond (Figure 3a), but the corresponding energy gain is compensated by the increase in energy arising from the approach of other atom pairs. Further reduction of R_{O-O} leads to an increase in the energy by ~3 kcal/mol and a distortion of the geometry near the hydrogen bond (Figure 3b). The transfer of the proton to the epoxy oxygen at fixed R_{O-O}

leads to a monotonic increase in the energy and is not a viable reaction path.

At this point, however, the PC oxygen can rotate around the epoxy O and move toward one of the two epoxy C atoms (R_{O-C} is an appropriate reaction coordinate). The energy increases very slowly up to a maximum of about 11.4 kcal/mol ($R_{O-O} = 2.5$ Å, $R_{O-C} = 2.2$ Å), while the OH group becomes parallel to the closest CO bond in the epoxy ring. The two epoxy C−O bonds are systematically slightly asymmetrical, the shorter bond being closest to the approaching OH. The distance between H and the epoxy O reduces slowly to ∼1.8 Å at the energy saddle point (Figure 3c). The reaction continues spontaneously to the structure shown in Figure 3d, with the simultaneous transfer of the proton to the epoxy O and the formation of a covalent bond between the epoxy C and the approaching O in the PC molecule. The overall reaction is exothermic, with a net energy gain of about 8 kcal/mol.

The changes in the total energy during the relaxation of the atomic positions at fixed reaction coordinate show that steric effects allow the reaction to proceed without a major energy increase *only* along a narrow valley in configuration space leading to the top of the reaction barrier. This geometry selectivity implies that the free energy barrier will be increased by entropy at any nonzero temperature above the barrier in the potential energy (11.4 kcal/mol). Tracking the minimum energy valley requires the approaching molecules to reorient during the reaction. Even though there is a significant change in the potential energy, these relaxations are relatively slow in our molecular dynamics approach, and the simulation of the central stage of the reaction was a major computational effort.

Simulation of three additional reaction paths confirms that CHO does not react readily with sites in the regular PC chain. The first tested the reactivity of the epoxy O with a phenol C atom that is not adjacent to the sp^3 oxygen, and we found no significant reorganization of bonds down to $R_{C-O} = 1.8$ Å, corresponding to an energy increase of more than 30 kcal/mol. The other two paths led to reactions at the carbonate group, the first of which inserts CHO between carbonate and the phenyl ring, using as reaction coordinate the distance between the epoxy O and the phenyl C bonded directly bonded to the carbonate. In this case there is also an increase in the energy to more than 30 kcal/mol without a significant change in the bonding pattern of the two approaching molecules.

A reaction with a barrier of slightly less than 30 kcal/mol occurs, however, if the epoxy O approaches the sp^2 C atom in the carbonate group. As illustrated in Figure 4, the orientation of CHO first changes such that its carbon backbone becomes nearly parallel to the carbonate plane (Figure 4a). A crucial step is the transformation of the carbonate geometry from cis−cis to trans−trans (Figure 4b), which occurs when the reaction coordinate is below 2 Å and the energy is above 15 kcal/mol. The transition state corresponds to a reaction coordinate of 1.52 Å and an energy of 28 kcal/mol (Figure 4c). In this configuration, the carbonate C is 4-fold coordinated with approximately tetrahedral geometry. The energy subsequently decreases to −8 kcal/mol by breaking an epoxy C−O bond and inserting CHO between carbonate and phenol (Figure 4d).

2. Trans Isomer of CHO (Figure 2d). The trans isomer of CHO has additional strain in its carbon backbone, and reactions at both the OH termination and the carbonate groups are exothermic with energy balances of 43 and 47 kcal/mol, respectively. Analysis of the charge distribution suggests that the reaction at the former may follow paths corresponding to reaction coordinates R_C with (a) the epoxy O approaching the hydroxyl H and (b) the hydroxyl O approaching the (positively charged) C_2 carbon of $C_6H_{10}O$.

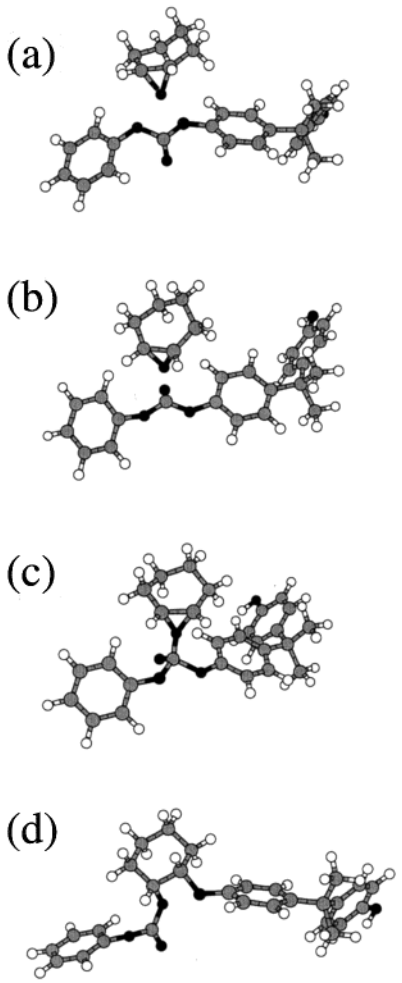

Figure 4. Reaction of the cis isomer of CHO with carbonate group of PC chain.

In the first case (Figure 5), a weak hydrogen bond forms in the direction of the epoxy−O (Figure 5a, $\Delta E = -2$ kcal/mol), followed by the transfer of the H atom (Figure 5b). The energy barrier is 18 kcal/mol, and the reaction proceeds by the unsaturated O atom moving toward one of the C atoms in the epoxy ring with very little change in energy. The breaking of one of the two epoxy C−O bonds (Figure 5c), releases a significant amount of potential energy, and the system reaches the final configuration (Figure 5d).

In the second case (Figure 6), reducing the distance between the hydroxyl O and one of the two C atoms in the epoxy ring leads to the simultaneous transfer of the *entire* phenoxide group to the C_2 carbon on the incoming $C_6H_{10}O$. The epoxy ring opens (Figure 6c), followed by the formation of the C−O bond between the two molecules (Figure 6d). The main relaxation is the reorientation of the O−H bond away from the positively charged C_2 atom (Figure 6b), and the energy barrier ($\Delta E = 38$ kcal/mol) is larger than in the previous case. The shortest C−O bond in the epoxy ring is the one that

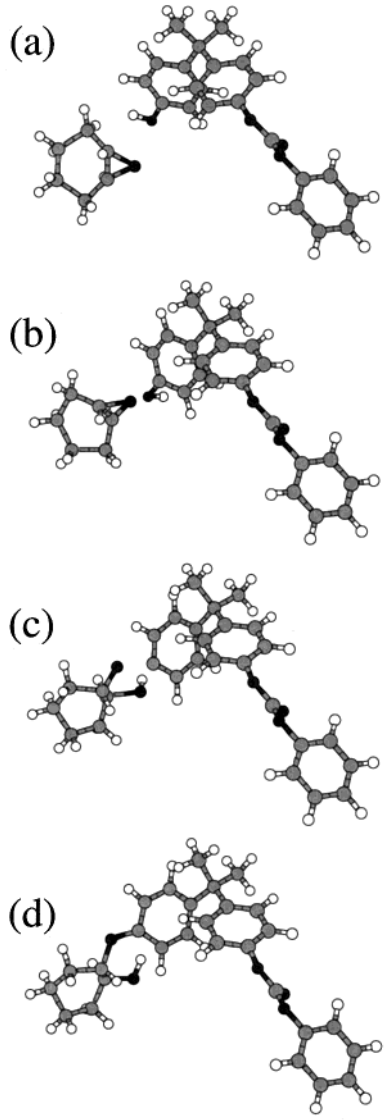

Figure 5. Reaction 1 of the trans isomer of CHO with OH termination.

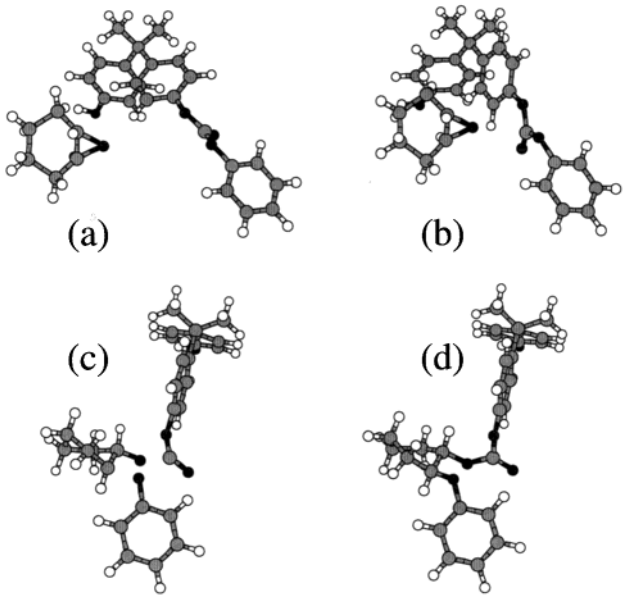

Figure 6. Reaction 2 of the trans isomer of CHO with OH termination.

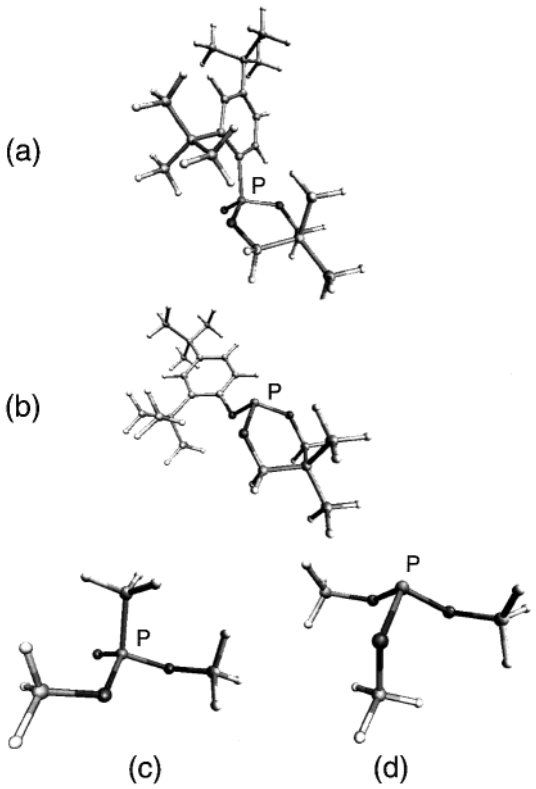

Figure 7. Phosphite molecules: (a,b) BPDD; (c,d) trimethyl phosphite, TMP.

eventually breaks in *both* simulations, which is further evidence for the substantial rearrangements that occur.

We note that the lower stability of the trans isomer of CHO is not reflected in a higher reactivity, but in a shift in the global energy balance. The same is true for the reaction of *trans*-CHO at the carbonate group that follows a trajectory similar to the one described for the cis isomer, overcoming a very similar potential energy barrier.

IV. Reaction of Phosphite Molecules with PC and Phenol

The main focus of our work on phosphite molecules has been 2-[2,4-bis(*tert*-butyl)phenoxy]-5,5-dimethyl-1,3,2- dioxaphosphorinane] (BPDD), which is shown in Figure 7b. This phosphite molecule with three single P−O bonds bears an obvious resemblance to the antioxidant tris(2,4-di-*tert*-butylphenyl) phosphite. In Figure 7a, we show the more stable phosphonate isomer with one P═O double bond (5,5-dimethyl-2-[2,4-bis(*tert*-butyl)phenyl]-1,3,2-dioxaphosphorinane-2-oxide). We have performed calculations for both structures and for the corresponding structures related to trimethyl phosphite (TMP) (Figure 7c,d), which is interesting in its own right and much simpler to study. The phosphonates (Figure 7a,c) are more stable than their phosphite counterparts, the energy differences being ΔE =10.6 kcal/mol in BPDD and 30.2 kcal/mol in TMP, including zero point energies.

The structural parameters, charges, dipole moments, and selected vibrational frequencies of all four molecules are given in Table 2. The obvious similarities between the structures of isomersshown in Figure 7a,c and in Figure 7b,d are reflected in the local environment of P and the corresponding atomic charges, particularly on the P atom.[18] Analysis of the vibrational frequency

Table 2. Bond Lengths (Å) and Angles (degrees), Atomic Charges (−*e*), Dipole Moments (D) and Vibrational Frequencies (cm^{-1}) Calculated for the Molecules in Figure 7

atoms	a	b	c	d
$P-O_1$	1.615	1.670	1.622	1.651
$P-O_2$	1.635	1.674	1.644	1.651
$P-O_3$	1.482	1.663	1.480	1.717
O_1-C_1	1.449	1.454	1.454	1.459
O_2-C_2	1.456	1.446	1.449	1.463
O_3-C_3		1.453		1.403
$P-C_3$	1.818		1.830	
O_1-P-O_2	101.7	91.3	104.2	103.3
O_1-P-O_3	112.8	103.3	113.1	101.8
O_2-P-O_3	115.7	103.4	114.0	99.2
O_1-P-C_3	106.7		110.7	
O_2-P-C_3	104.4		101.4	
O_3-P-C_3	114.3		112.5	
$Q(P)$	0.88	0.02	0.84	−0.03
$Q(O_1)$	−0.32	−0.19	−0.36	−0.23
$Q(O_2)$	−0.29	−0.18	−0.39	−0.22
$Q(C_3)$	−0.59	−0.20	−0.59	−0.14
$Q(C_1)$	−0.08	−0.03	0.13	0.04
$Q(C_2)$	−0.10	0.02	0.01	−0.01
$Q(C_3)$	−0.39	−0.05	0.01	0.22
dipole	4.83	1.31	5.51	3.35
P−O stretch	790−810	720−800	790−810	740−810
P═O stretch	1260−1290		1250−1260	
C−O stretch	1010−1050	990−1060	1030−1110	1030−1100, 1210−1230
P−C stretch	689		673	
PO_3 breath		559		629

modes reveals characteristic stretching modes of PO_3 and P−C structural units for isomers shown in Figure 7a,c, and a breathing mode of the PO_3 unit for isomers shown in Figure 7b,d.

A. Reactions of BPDD with PC. We first describe the insertion of the isomer of BPDD shown in Figure 7b into the PC chain as modeled by DPC-plus. This isomer is less stable and presumably more reactive than that shown in Figure 7a, and the existence of butyl group branches allows us to study steric hindrance effects. As in the case of CHO, the reactions were tested at (a) the OH termination and (b) the carbonate group of DPC-plus. Snapshots of the reactions are shown in Figures 8 and 9, with the reaction coordinates being the distances between the phosphite P and (a) hydroxyl O and (b) carbonate C, respectively.

In both reactions, there is initially a weak bond between the reactant molecules (the minimum energies at a separation of 4 Å are −1.6 and −3.7 kcal/mol, respectively). However, from Figure 8b (R_C = 3.0 Å, E = −0.1 kcal/mol) and Figure 9b (R_C = 3.5 Å, E = −3.5 kcal/mol), the total energy rises rapidly as the separation between the molecules decreases. At this point in the second reaction the carbonate group, which tilted toward P on bringing the carbonyl O closer, begins to bend back. Although we now adopted a different R_C (the distance between the phosphite P and the carbonyl O), it is clear that neither reaction is favored, the energies being 31.0 and 18.5 kcal/mol at 2 Å in Figures 8c and 9c, respectively. In both cases, substantial structural rearrangements resulted in PO_4 entities with near-linear O−P−O bonds, but neither structure corresponds to a local minimum in the energy surface. Reaction b was repeated with the PO_4 unit initially in a tetrahedral configuration, but energy optimization led to the same PO_4 form.

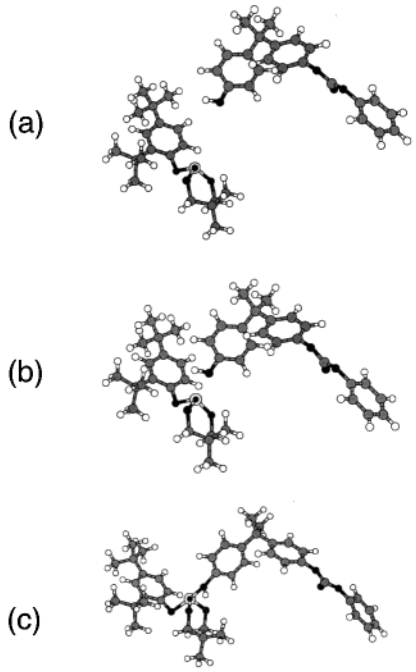

Figure 8. Reaction of phosphite group of BPDD with OH termination. The P atom is denoted by a larger sphere with a dot.

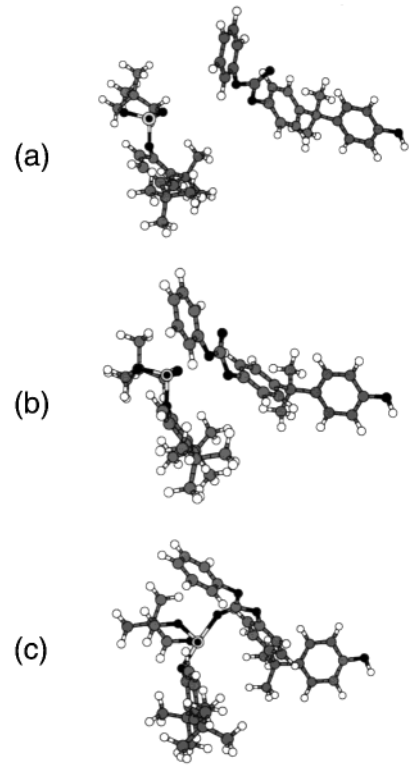

Figure 9. Reaction of phosphite group of BPDD with carbonate group of PC. The P atom is denoted by a larger sphere with a dot.

B. Reaction of TMP with Phenol. It is natural to ask whether the essential features of the reactions can be reproduced by considering smaller molecules, and we have studied reactions between phenol (the termination of the DPC-plus segment) and both trimethyl phosphite and its phosphonate isomer.

The reaction between the phosphite form (Figure 7d) and phenol proceeds in a fashion similar to that shown in Figure 8. With R_C taken to be the distance between

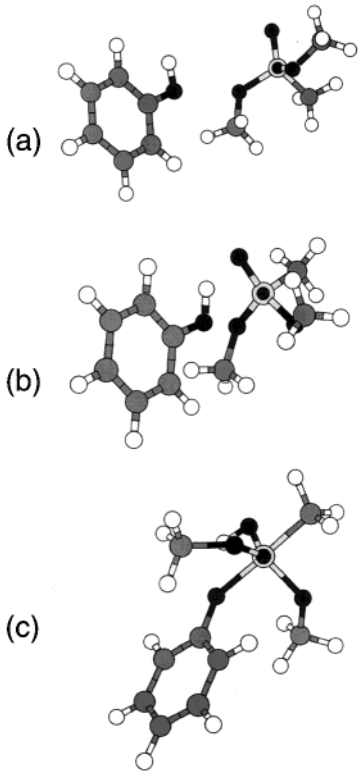

Figure 10. Reaction of trimethyl phosphite with phenol. The P atom is denoted by a larger sphere with a dot.

P and the phenol O, the energy initially falls slightly and then rises to 8.1 kcal/mol for $R_C = 2.5$ Å. When $R_C = 2.0$ Å ($E = 27.6$ kcal/mol), the "seesaw" structure with a linear O−P−O beam is evident. The reactivity of the phosphonate (Figure 7c) has also been studied, with R_C chosen to be the distance between the P and hydroxyl O, and snapshots of this reaction are shown in Figure 10. The molecules tilt initially due to the formation of a hydrogen bond between the hydroxyl H and double-bonded O in the phosphite group (the lowest energy of −5.3 kcal/mol corresponds to a hydrogen bond length 1.77 Å and $R_C = 3.0$ Å). In Figure 10b ($R_C = 2.7$ Å, $E = -0.75$ kcal/mol) the bending and compression of hydrogen bond contribute to a rapid increase in energy to 26.7 kcal/mol ($R_C = 2.1$ Å), where the hydroxyl H transfers to the phosphite O.

Relaxation of this configuration leads to a stable minimum in the energy surface (Figure 10c, $R_C = 1.84$ Å) 17.8 kcal/mol above the initial energy, i.e., the reaction is strongly endothermic. There is an obvious analogy to the PO_4 unit mentioned above, as we also find a tendency to form a linear bond, in this case O−P−C. The three P−O bonds are arranged almost symmetrically in the plane perpendicular to the O−P−C bond, and the large effective charge $Q(P) = 1.13$ reflects the 5-fold coordination of the P atom.

The seesaw structure of the PO_4 unit has occurred repeatedly in the present calculations, and we have performed calculations of charged and neutral PO_4H_4 molecules. While $PO_4H_4^+$ occurs in a stable tetrahedral form (Figure 11a), the only structure of PO_4H_4 that is a stable minimum (i.e., having all vibration frequencies real) is the seesaw form shown in Figure 11b. There are four bonding orbitals on the P atom, and the unbound HOMO is much (more than 3 eV) higher in energy and has a large weight in the region above the fulcrum of the seesaw. A phosphoranyl radical ($^{\bullet}P(OMe)_4$) with an

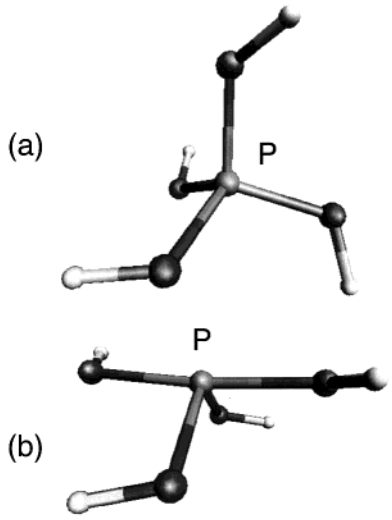

Figure 11. Stable isomers of (a) $PO_4H_4^+$ and (b) PO_4H_4.

analogous structure has been observed in electron spin resonance measurements.[19] On the other hand, tetrahedral configurations are observed in a similar context, namely structures found during a mass spectrometric and DF study of the reaction of the phosphonium cation $(HO)_2P{=}O^+$ with methanol.[20]

V. Discussion and Concluding Remarks

Epoxides and phosphites are important additives in the production of polycarbonates, and we have performed density functional (DF) calculations for the reactions of both types of molecule with segments of PC chains. We have focused on possible courses of reactions between isomers of both cyclohexene oxide (CHO, cyclohexane epoxide) and phosphite molecules with two sites on the PC chain, the carbonate group and a prototypical defect, the OH termination. Although the computational demands mean that only a selection of possible reactions can be studied, the results provide further evidence that detailed information can be obtained about the energy surfaces of complex reactions involving over 100 atoms.

In the case of CHO, we have identified reaction paths with modest reaction barriers in all cases: The epoxide ring opens, barriers of ∼10 kcal/mol must be surmounted, and the overall reactions are exothermic. A comparison of the reactions of two isomers of CHO with the OH-terminated chain shows the expected importance of steric effects. The energy surfaces found in the case of phosphite molecules are different. In all cases the energy increases as the reactants approach each other, and the final structure resembles a seesaw with the P atom at the center of a linear arrangement of three atoms. The phosphonate isomer also shows no tendency to react.

It is natural to speculate on the reasons for the absence of reactions in phosphites, which are common additives in the manufacture of polymers. The stabilization of polymer processes and properties is usually achieved by the use of several additives, and individual components might require the presence of other additives to be effective. It is possible that phosphite molecules could be oxidized to phosphate before the reaction with PC can take place or that the reaction between phosphite and PC takes place at another point in the PC chain. There are also severe restrictions

imposed at present by DF calculations on systems of this complexity, including the requirements that the system remains in its ground state throughout the reaction and has a definite spin state. While we may be able to choose likely candidates for a reaction and the path it might take, an exhaustive treatment of *all* conceivable processes is presently impossible.

Acknowledgment. This work was supported by the Bundesministerium für Bildung and Forschung, Bonn (BMBF-Kompetenzzentrum Werkstoffmodellierung, 03N6015) and by Bayer AG, Leverkusen, Germany. J.A. thanks the Academy of Finland and the Väisälä Foundation, Helsinki, for financial support. We thank F. Bruder and S. Kratschmer for suggesting these calculations and for helpful discussions, and W. Ebert and M. Möthrath (all Bayer, Uerdingen, Germany) for comments on the original manuscript. The calculations were performed on Cray T3E computers in the Forschungszentrum Julich with generous support of the Forschungszentrum and the John von Neumann Institute for Computing (NIC).

References and Notes

(1) See, for example: Hutnik, M.; Argon, A. S.; Suter, U. W. *Macromolecules* **1991**, *24*, 5970. Tomaselli, M.; Robyr, P.; Meier, B. H.; Grob-Pisano, C.; Ernst, R. R.; Suter, U. W. *Macromolecules* **1996**, *29*, 1663. Goetz, J. M.; Wu, J.; Yee, A. F.; Schaefer, J. *Macromolecules* **1998**, *31*, 3016 and references therein.

(2) Montanari, B.; Ballone, P.; Jones, R. O. *Macromolecules* **1998**, *31*, 7784.

(3) Montanari, B.; Ballone, P.; Jones, R. O. *Macromolecules* **1999**, *32*, 3396.

(4) Ballone, P.; Montanari, B.; Jones, R. O. *J. Phys. Chem. A* **2000**, *104*, 2793.

(5) Ballone, P.; Jones, R. O. *J. Phys. Chem. A* **2001**, *105*, 3008.

(6) See, for example, *Plastics Additives Handbook*, 4th ed.; Gächter, R., Müller, H., Eds.; Hanser: New York, 1993.

(7) Borrmann, A.; Montanari, B.; Jones, R. O. *J. Chem. Phys.* **1997**, *106*, 8545.

(8) Montanari, B.; Jones, R. O. *Chem. Phys. Lett.* **1997**, *272*, 347.

(9) Troullier, N.; Martins, J. M. *Phys. Rev. B* **1991**, *43*, 1993.

(10) Perdew, J. P.; Burke, K.; Ernzerhof, M. *Phys. Rev. Lett.* **1996**, *77*, 3865.

(11) Hutter, J.; et al. CPMD program version 3.0. Max-Planck-Institut für Festkörperforschung and IBM Research, 1990−1999.

(12) Ikeda, T.; Kewley, R.; Curl, R. F., Jr. *J. Mol. Spectrosc.* **1972**, *44*, 459 (microwave spectrum).

(13) Traetteberg, M.; Sandnes, T. W.; Bakken, P. *J. Mol. Struct.* **1980**, *67*, 235 (electron diffraction).

(14) Pawar, D. M.; Noe, E. A. *J. Am. Chem. Soc.* **1998**, *120*, 1485.

(15) Past experience indicates that bond lengths are accurate to better than 0.01 Å, and bond angles to better than 1°. The inclusion of values to within 0.001 Å and 0.1° should be taken to imply that the results are more reliable than those with one decimal place less.

(16) See, for example, Morrison, R. T.; Boyd, R. N. *Organic Chemistry*, 6th ed.; Prentice Hall: Englewood Cliffs, NJ, 1992; pp 713−721.

(17) See, for example, Holder, A. J.; Morrill; White, D. A.; Eick, J. D.; Chappelow, C. C. *J. Mol. Struct. (THEOCHEM)* **2000**, *507*, 63.

(18) The effective charges are determined by fitting the electrostatic potential of the molecules.

(19) McConnachie, G. D. G.; Rai, U. S.; Symons, M. C. R. *J. Mol. Struct.* **1993**, *300*, 527.

(20) Gevrey, S.; Luna, A.; Taphanel, M.-H.; Tortajada, J.; Morizur, J.-P. *Int. J. Mass Spectrom.* **2000**, *195/196*, 545.

MA011757T